



# Estimating human long bone cross-sectional geometric properties: a comparison of noninvasive methods

Matthew C. O'Neill\*, Christopher B. Ruff

*Center for Functional Anatomy and Evolution, Johns Hopkins University School of Medicine,  
1830 E. Monument St., 3<sup>rd</sup> Floor, Baltimore, MD 21205*

Received 6 November 2003; accepted 12 July 2004

---

## Abstract

Cross-sectional properties (areas, second moments of area) have been used extensively for reconstructing the mechanical loading history of long bone shafts. In the absence of a fortuitous break or available computed tomography (CT) facilities, the endosteal and/or periosteal boundaries of a bone may be approximated using alternative noninvasive methods. The present study tests whether cross-sectional geometric properties of human lower limb bones can be adequately estimated using two such techniques: the ellipse model method (EMM), which uses biplanar radiography alone, and the latex cast method (LCM), which involves molding of the subperiosteal contour in combination with biplanar radiography to estimate the contour of the medullary canal. Results of both methods are compared with “true” cross-sectional properties calculated by direct sectioning. The study sample includes matched femora and tibiae of 50 Pecos Pueblo Amerindians. Bone areas and second moments of area were calculated for the midshaft femur and tibia and proximal femoral diaphysis in each individual. Percent differences between methods were derived to evaluate directional (systematic) and absolute (random) error. Multiple regression was also used to investigate the sources of error associated with each method.

The results indicate that while the LCM shows generally good correspondence to the true cross-sectional properties, the EMM generally overestimates true parameters. Regression equations are provided to correct this overestimation, and, when applied to another sample, are shown to significantly improve estimates for the femoral midshaft, although corrections are less successful for the other section locations. Our results suggest that the LCM is an adequate substitute for estimating cross-sectional properties when direct sectioning and CT are not feasible. The EMM is a reasonable alternative, although the bias inherent in the method should be corrected

---

\* Correspondence to: Matthew C. O'Neill, Center for Functional Anatomy and Evolution, Johns Hopkins University School of Medicine, 1830 E. Monument St., 3<sup>rd</sup> Floor, Baltimore, MD 21205. Tel: +1 443 287 3901; fax: +1 410 614 9030.

*E-mail addresses:* [moneill9@jhmi.edu](mailto:moneill9@jhmi.edu) (M.C. O'Neill), [cbruff@jhmi.edu](mailto:cbruff@jhmi.edu) (C.B. Ruff).

if possible, especially when the results of the study are to be compared with data collected using different methods.

© 2004 Elsevier Ltd. All rights reserved.

*Keywords:* cross-sectional geometry; femur; tibia; human; biomechanics

---

## Introduction

Long bone diaphyseal cross-sectional properties (areas, second moments of area) have been used to address a variety of issues in human skeletal adaptation, including the evolution of locomotor performance and manipulative behavior, changes in skeletal structure during growth and development, and the effects of subsistence strategy on behavioral patterns (e.g., Ruff et al., 1993, 1994; Trinkaus et al., 1994; Ruff, 1999; Trinkaus et al., 1999; Stock and Pfeiffer, 2001; Holt, 2003; Ruff, 2003b, c). These studies have been facilitated by the development of more automated techniques for deriving section properties from image data, such as SLICE (Nagurka and Hayes, 1980). However, any such analysis is still dependent on obtaining accurate bone cross-sectional images. Fortuitous breaks or physical sectioning of specimens allow direct measurement of image contours, but in most cases a noninvasive method must be used. Although computed tomography (CT) is the method of choice for this (Sumner et al., 1985), CT scanning may not always be feasible due to problems of access or cost constraints. Biplanar radiography, alone or in combination with direct measurement of external bone contours, has been the most commonly used alternative (Trinkaus and Ruff, 1989; Fresia et al., 1990; Ruff, 1995; Runestad, 1997; Sakaue, 1998; Trinkaus and Ruff, 1999a,b; Churchill and Smith, 2000; Connour et al., 2000). This noninvasive approach has been shown to provide reasonably accurate results in some samples (Ruff, 1989; Fresia et al., 1990; Runestad et al., 1993; Stock, 2002); however, it has not been systematically tested on human lower limb bone remains, despite the fact that they are the most commonly included skeletal elements in cross-sectional analyses (see references above).

The two methods evaluated in this study will be referred to as the ellipse model method (EMM) and the latex cast method (LCM), following Stock (2002). For the EMM, radiographs taken in any number of planes may be used to reconstruct internal bone contours (Ruff, 1989, 1995), but biplanar radiographs taken in anteroposterior (A-P) and mediolateral (M-L) planes are most frequently employed. Modeling the cortex as two ellipses, subperiosteal and endosteal breadths measured on the A-P and M-L radiographs can be used to calculate section properties using standard geometric formulae (Runestad et al., 1993; see below). In its simplest form, the EMM assumes that the two ellipses are concentric, i.e., have the same centers of area. In a more complex derivation of this model, the parallel axis theorem is used to place the centroid of the internal ellipse eccentrically within the external ellipse (Biknevicius and Ruff, 1992; Ohman, 1993; Runestad et al., 1993; Lazenby, 1997, 1998; Stock, 2002). However, differences between results of the eccentric ellipse model and the concentric model are relatively small (Ohman, 1993; Runestad et al., 1993; Lazenby, 1997, 1998), except in sections with very asymmetric cortical thickness, such as the mandibular corpus (Biknevicius and Ruff, 1992). For this reason, the concentric EMM will be the focus of this study.

For the LCM, the actual subperiosteal contour is obtained by placing molding material around the section of interest (although other techniques may be used; see Materials and Methods), and only the medullary cavity is reconstructed from biplanar radiographs (A-P and M-L). The LCM exploits the mechanical principle that, in a beam experiencing bending and/or torsional loading, the material furthest from the section centroid is the most relevant for providing rigidity and strength (Wainwright et al., 1978). Thus, accurate

reconstruction of the subperiosteal contour is more important than accurate reconstruction of the endosteal contour in determining biomechanically relevant properties. This method in particular has been used frequently in comparative studies of fossil hominin bone rigidity/strength (e.g., Churchill, 1994; Trinkaus, 1997; Trinkaus et al., 1998a,b; Trinkaus and Ruff, 1999a,b).

The purpose of the present study is to examine the accuracy of the EMM and LCM for estimating cross-sectional geometric properties of human lower limb bones. Long bone dimensional data, obtained from radiographs and external contours available as part of a previous study of an archaeological skeletal sample (Ruff and Hayes, 1983a,b), were used to calculate section properties using the two noninvasive estimation methods. These data were compared to the “true” cross-sectional properties of the same bones that were collected by direct sectioning during the original study. The errors associated with the EMM and LCM were evaluated using several techniques, and possible sources of error were investigated. Based on these results, we present bivariate regression equations that can be used for correcting radiographically derived estimates, and test them using independent samples of human long bones.

## Materials and Methods

Cross-sectional geometric properties were collected from the lower limb bones of a sample of adult Amerindians from Pecos Pueblo, New Mexico. The provenience of the Pecos Pueblo skeletal collection has been described in detail in several previous publications (Hooton, 1930; Kidder, 1958; Ruff and Hayes, 1983a,b). Briefly, Pecos Pueblo was a large late prehistoric and protohistoric site in north-central New Mexico with an agricultural subsistence base. Sexing and aging of individuals were carried out as described previously (Ruff, 1981). Right or left femora and tibiae (both bones from the same side) were sectioned, and digitized photographs of these sections were used to determine cross-sectional properties (Ruff and Hayes, 1983a). Prior to sectioning, biplanar radiographs were taken of

each bone in standardized A-P and M-L planes (Ruff and Hayes, 1983a). Radiographs from 50 individuals (29 males, 21 females) were used here for collecting the noninvasive property estimates.

Five diaphyseal sections on each bone, based on percentages of a bone length dimension [biomechanical length' (Ruff and Hayes, 1983a)], were originally measured on this sample. However, only the three section locations most often used in comparative biomechanical studies (e.g., Trinkaus, 1997; Trinkaus et al., 1998a,b; Trinkaus and Ruff, 1999a,b; Stock and Pfeiffer, 2001; Holt, 2003) were included here. These are at 80% (subtrochanteric) and 50% (midshaft) of bone length' from the distal end of the femur, and at 50% (midshaft) of bone length' for the tibia. To measure cross-sectional breadths from radiographs, a clear acetate template marked with longitudinal and transverse lines was placed over each radiograph, aligned with the long axis of the diaphysis, and positioned so that the transverse line corresponded to the correct section as described above. Total subperiosteal, medullary, and cortical breadths were then measured using digital calipers to the nearest 0.01 mm along the transverse line (Fig. 1). Measurement repeatability was assessed through remeasurement of five individuals several weeks after the original measurements were taken. The mean difference between measurements was 0.7% for subperiosteal breadths, 3.0% for medullary breadths, and 4.4% for cortical breadths. Radiographic enlargement (parallax), which averaged 5.6%, was determined by comparing radiographic with direct measurements (taken on the intact bones in the original study) of subperiosteal breadths, and corrected in all radiographic breadth dimensions.

Subperiosteal contours used in the LCM are usually derived from molds made from a silicon putty material placed around the bone at the section of interest, allowed to harden, then removed (cut off) and traced (e.g., Trinkaus and Ruff, 1989). However, because no molds were taken of the Pecos material during the original study, and the sample has since been repatriated, an alternative, but equivalent, approach was used here. The original photographs of the cut sections were scanned into the program NIH Image

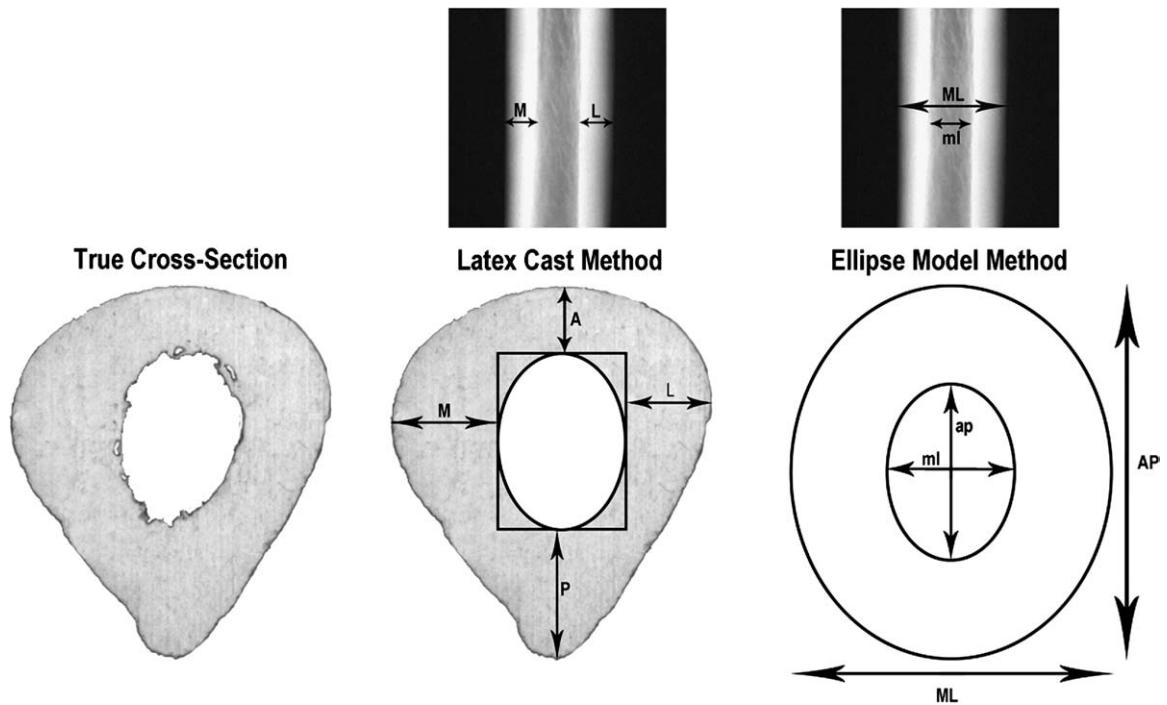


Figure 1. Diagrams of the measurements used to reconstruct a long bone cross-section using the LCM and EMM. For the LCM, subperiosteal contours were directly measured and cortical breadths derived from radiographs were used to reconstruct the medullary cavity. The section was then entered into a geometric analysis program (see text). For the EMM, total subperiosteal and medullary breadths were both measured from radiographs and used to calculate section properties using the formulae in Table 1. Only A-P radiographs are shown for illustration, although radiographs in both A-P and M-L planes were measured.

(version 1.62), and the medullary cavities were completely filled in using the “paint tool” function. The remaining subperiosteal contours were then used in the LCM as described below. The equivalence between this and the more traditional latex casting method was tested using an independent sample ( $n = 10$  individuals) of Predynastic Egyptian femora (Zabecki et al., 2004) for which broken ends (all approximately midshaft sections) could be both photographed and molded. For each section, photographs and subperiosteal latex casts were taken, and then used to compute total subperiosteal area and an index of cross-sectional shape ( $I_{\max}/I_{\min}$ ) determined using the subperiosteal perimeter alone. There was no significant difference between the estimates of total area (paired  $t$ -test,  $p = 0.246$ ) or cross-sectional shape ( $p = 0.726$ ) generated by the photographic and casting approaches. This confirms that the

photographic approach employed in this study provides a reconstruction of the subperiosteal perimeter not significantly different from that of a latex cast, and demonstrates that any error inherent in the LCM will be almost entirely due to interpolation of the medullary cavity.

The three cross-sectional reconstruction techniques—true, EMM, and LCM—are illustrated in Figure 1. For the EMM estimations, A-P and M-L subperiosteal and medullary breadths measured from the radiographs were simply entered into the formulae shown in Table 1. (Only second moments of area in the radiographic planes, and not maximum and minimum second moments of area, can be determined using the EMM.) For the LCM, A-P and M-L cortical breadths were measured inward from the (true) subperiosteal surface and used to reconstruct an elliptical medullary cavity. It is important to note that, because a radiographic

Table 1

Equations for calculation of cross-sectional geometric properties for the ellipse model method (EMM)

Cross-sectional property	Equation	Mechanical interpretation
Total area	$TA = \pi \cdot [(AP \cdot ML)/4]$	
Medullary area	$MA = \pi \cdot [(ap \cdot ml)/4]$	
Cortical area	$CA = \pi/4 \cdot [(AP \cdot ML) - (ap \cdot ml)]$	Resistance to axial (tension or compression) loads <sup>a</sup>
Second moment of area about M-L (x) axis	$I_x = \pi/64 \cdot [(AP^3 \cdot ML) - (ap^3 \cdot ml)]$	Bending rigidity in the AP plane <sup>a</sup>
Second moment of area about A-P (y) axis	$I_y = \pi/64 \cdot [(AP \cdot ML^3) - (ap \cdot ml^3)]$	Bending rigidity in the ML plane <sup>a</sup>
Polar second moment of area	$J = I_x + I_y$	Summed bending rigidity in the AP and ML planes or torsional rigidity <sup>a</sup>

<sup>a</sup> Section moduli, measures of bending/torsional strength, can be determined by dividing second moments of area by half the appropriate cross-sectional diameter or by taking the second moment of area to the power 0.73 (Ruff, 2000).

image compresses three-dimensional morphology into a two-dimensional representation, the cortical breadths measured from the radiographs may not be collinear when applied to the subperiosteal contour since breadths must be measured inward from the most projecting point on each side of the section (see Fig. 1). Once the anterior, posterior, medial, and lateral limits of the medullary cavity were defined, the cavity was reconstructed as an ellipse, using the subperiosteal border as a guide. Each reconstructed cross-sectional image was then analyzed using a modified version of NIH Image (version 1.62) that includes a macro for calculating geometric section properties. This program is available from the authors at: <http://www.hopkinsmedicine.org/FAE/CBR.htm>.

The comparability of the two noninvasive estimates with true cross-sectional properties was evaluated using several methods. Most analyses included only cortical area and second moments of area, as these are the most critical properties in terms of bone rigidity/strength evaluations; however, mean prediction errors were calculated for total subperiosteal and medullary areas as well. The possibility of size dependence of estimation errors was tested by fitting regression lines through bivariate data scatters of estimated against true values for all sections combined and testing the slopes against isometry (1.0). Regression statistics were generated on log-transformed data in order to correct for heteroscedasticity among the raw values. Correlation coefficients and percent standard errors of estimate (%SEE) were used to assess the tightness of these bivariate scatters.

Mean directional ( $[(\text{estimate} - \text{true})/\text{true}] \times 100$ ) and absolute ( $|(\text{estimate} - \text{true})/\text{true}| \times 100$ ) percent

prediction errors between raw values from the true and noninvasive estimates were calculated for each technique, property, and section independently. The directional and absolute errors can be taken as representative of the systematic and random biases, respectively, of each method. For directional prediction errors, negative values indicate that the method underestimated the true section properties, while positive values indicate an overestimate. The percent prediction errors, and accompanying paired *t*-tests, were the primary methods used to evaluate the accuracy and reliability of the noninvasive techniques. This approach is comparable to the “assessment of agreement” proposed by Altman and Bland (1983) and Bland and Altman (1986) in that it provides a test of the accuracy of an estimate independent of the regression statistics.

To further investigate potential sources of estimation error, a multiple regression of true section properties against the estimated properties plus sex, age, and several skeletal morphological characteristics was carried out. Following the original analysis of this sample (Ruff and Hayes, 1983b), ages were grouped into five-year intervals between 20 and 49 years, and a 50 + year category. All continuous variables were transformed to natural logarithms. The additional skeletal parameters included: a) the percent cortical area of the section (%CA), calculated as (cortical area/total area)  $\times$  100, an index of relative cortical thickness; b) the ratio of maximum to minimum second moments of area ( $I_{\max}/I_{\min}$ ), an index of bone shape; and c) the orientation of greatest bending rigidity [ $\theta$ ], a measure of section orientation relative to A-P and M-L axes. In addition, bone length was

included in the multiple regression to further assess the effects of body size on estimation errors. Because the sample is from a single, homogeneous population, the potential pitfalls of using bone lengths as body size surrogates (e.g., those associated with interpopulational differences in limb proportions) are minimized.

Finally, based on our results, ordinary least squares regression equations were generated to correct radiographic (EMM) estimates for each section (LCM estimates were found to be very close to true values, so no correction formulae were derived for these) (Smith, 1994). These equations were tested by applying them to two independent samples: a sample of Amerindian femora from the Georgia coast (Ruff et al., 1984), and a sample of modern U.S. white tibiae (Ruff and Hayes, 1988) (both  $n = 10$  individuals). All statistical analyses were carried out using SPSS 10.0 and SYSTAT 8.0.

## Results

Bivariate scatter plots of the estimated against true properties for the pooled femoral and tibial sections are shown in Figure 2 for cortical area and second moments of area. Associated regression statistics are given in Table 2. Correlations between estimated and true values are quite high, ranging from 0.92 to 0.99 for the LCM and from 0.92 to 0.95 for the EMM. Percent standard errors of estimate are generally low for the LCM, ranging between 4–9% for most properties (except MA, which is about 16%), and are higher for the EMM, ranging between 7–16%. Overall, the EMM technique overestimates true cross-sectional properties while the LCM estimates show good correspondence with true values (Fig. 2). Regression slopes (Table 1) indicate little size effect on estimation errors: although some least squares regression slopes are statistically significantly different from 1.0, all slopes are actually close to this value (0.92–1.02). Following previous researchers (Lazenby, 1998, 2002; Stock, 2002), reduced major axis (RMA) slopes were also calculated, and these are almost all extremely close to, and nonsignificantly different from, 1.0 (Table 2).

Mean directional and absolute percentage errors for each technique and all section properties and locations are shown in Table 3. These generally confirm the previous results. For the EMM, directional errors average 3–10% and, although they vary by section, most properties are overestimated. The only exceptions to this are the medullary area (MA) estimates, which are consistently underestimated across femoral and tibial sections. For the LCM, the directional percent errors are much lower, averaging 1–4%, except for femoral MAs, which are more strongly underestimated. Similarly, the absolute (random) errors are higher for the EMM, averaging 5–12%, than for the LCM, which averaged 3–8% (again, except for MA estimates, where errors were higher).

The results of the multiple regression analyses are shown in Tables 4 and 5. For the EMM (Table 4), none of the variables are significant predictors of error for the femur 50% section, while for the femur 80% section, the  $I_{\max}/I_{\min}$  ratio is a significant predictor of error in estimates of cortical area and second moments of area. In the tibia 50% section, several variables contribute to estimation error for CA and  $I_y$ , including sex, %CA,  $I_{\max}/I_{\min}$  (CA only), and theta. Because theta in the midshaft tibia is not far from A-P (Ruff and Hayes, 1983a), the negative slopes in Table 4 indicate that a greater departure from an A-P oriented section is associated with more error. For the LCM (Table 5), only one variable, femur length, is a significant predictor of error (for  $I_y$ ) in the femur 50% section. In the femur 80% section, theta is the most significant predictor for all of the properties examined. Here, the average orientation of theta is slightly closer to M-L (Ruff and Hayes, 1983a), so that the positive slopes indicate, again, a greater departure from an “anatomical” (in this case, M-L) axis. Percent cortical area (%CA) and  $I_{\max}/I_{\min}$  are also significant error predictors for CA. In the tibia 50% section, %CA is a significant error predictor for CA,  $I_y$ , and J, but not  $I_x$ . This is similar to the result from the analysis of EMM error (Table 4); the negative slopes suggest that thin cortices in the tibia increase estimation error. For  $I_y$  and J, theta also affects the estimation error. Finally, for CA, tibia length contributes significantly to the error in estimation.

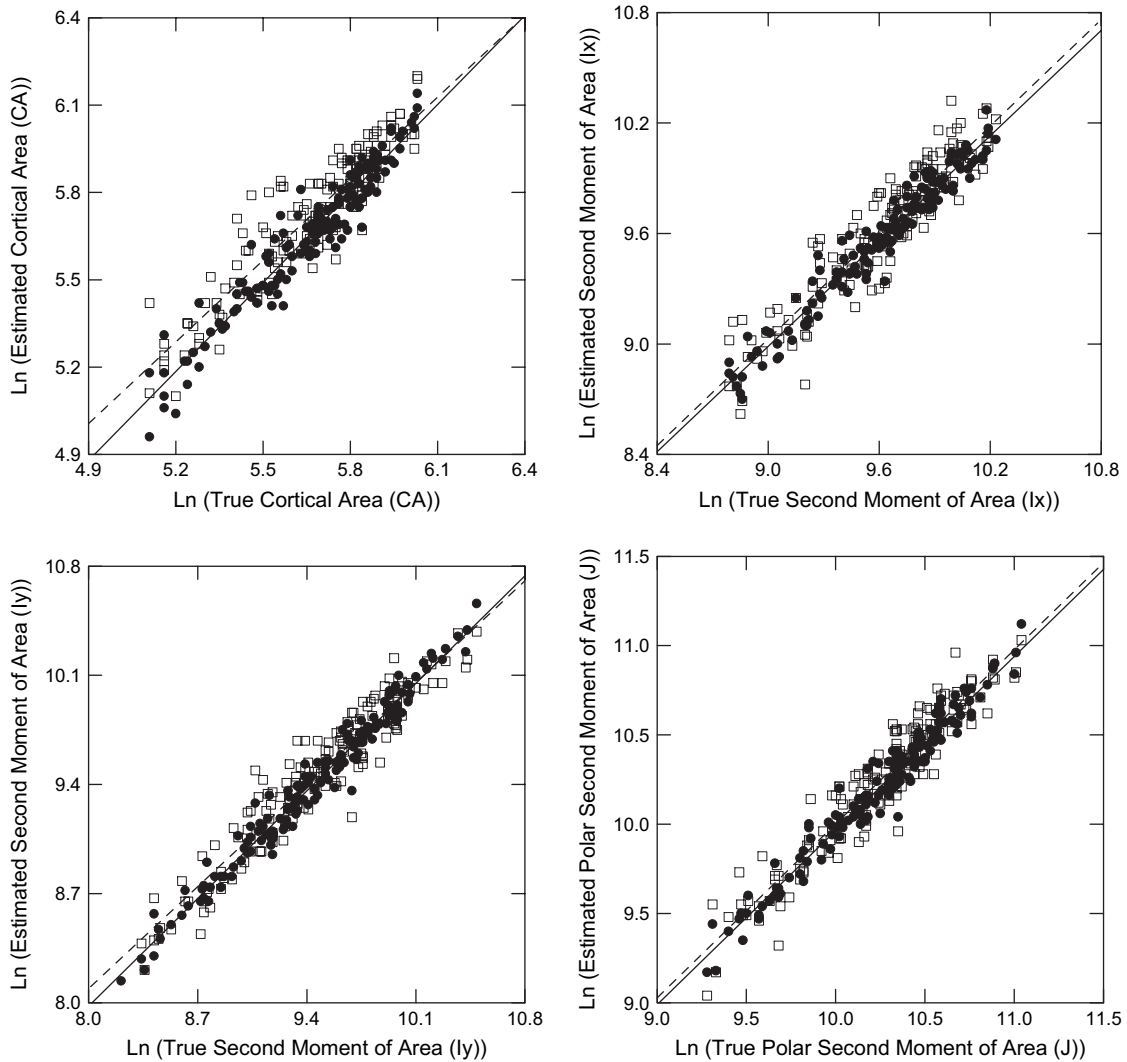


Figure 2. Scatter plots of pooled (i.e., femur 50%, 80%, and tibia 50% sections) true cross-sectional properties (areas, second moments of area) against values estimated using the EMM (squares) and the LCM (solid circles). All data transformed to natural logarithms. Ordinary least squares regression lines through the EMM (dashed lines) and LCM (solid lines) are shown. Equivalence between the true and estimated properties would be indicated by a line drawn between the lower left and upper right corners.

Least squares correction formulae for areas and second moments of area calculated using the EMM are given for each section in Table 6, along with the effects of applying these equations to the test samples. Original estimates and corrected values are shown graphically in Figure 3 for CA and J. On average, the correction equations improve the EMM cross-sectional property estimates, reducing directional errors from an average

of 12.2% to an average of 5.8%. However, the degree of improvement varies by section and property. The most substantial error reduction is in the femur 50% section, where EMM errors originally ranged from 13–18% and were reduced to 0–4%. Maximum individual errors in this section are also reduced from 30% or more to less than 17%. Error in cortical area estimation in the femur 80% and tibia 50% sections is also

Table 2

Pooled section regression equations for the latex cast method (LCM) and the ellipse model method (EMM)

	LCM					EMM				
	r	OLS <sup>a</sup>	RMA <sup>b</sup>	SE <sup>c</sup>	%SEE <sup>d</sup>	r	OLS <sup>a</sup>	RMA <sup>b</sup>	SE <sup>c</sup>	%SEE <sup>d</sup>
TA	0.98	0.96*	0.98	0.015	3.9	0.94	0.93*	0.99	0.027	7.0
MA	0.92	0.92**	1.00	0.033	15.6	0.95	0.94*	0.99	0.025	11.8
CA	0.96	1.02	1.06*	0.024	6.7	0.92	0.93*	1.01	0.034	9.5
I <sub>x</sub>	0.97	0.95*	0.98	0.018	8.2	0.93	0.97	1.04	0.032	14.9
I <sub>y</sub>	0.99	0.98	0.99	0.014	4.7	0.96	0.95*	0.99	0.024	15.7
I <sub>max</sub>	0.98	0.97	0.99	0.017	8.5	—	—	—	—	—
I <sub>min</sub>	0.99	1.00	1.01	0.014	8.7	—	—	—	—	—
J	0.98	0.98	1.00	0.017	8.2	0.95	0.98	1.03	0.027	13.7

*P*-value significant at \* $\alpha = 0.05$  and \*\* $\alpha = 0.01$ , comparisons with isometry (1.0).

<sup>a</sup> Ordinary least-squares slope.

<sup>b</sup> Reduced major axis slope.

<sup>c</sup> Standard error of the slope (same for OLS and RMA).

<sup>d</sup> Percent standard error of the estimate for the OLS regression equations.

substantially reduced, from means of 10–17% to 1–5%, and maximum individual errors of 18–30% to 10–20%. However, error reduction in most other section properties is either marginal or nonexistent, with EMM errors in some properties, such as the femur 80% I<sub>x</sub> and J, actually increasing after correction.

## Discussion

The generally strong correlations, low standard errors, and low directional bias of the LCM results compared to true section properties support its continued use as a robust noninvasive approach to collecting cross-sectional properties of human long

Table 3

Directional and absolute percent errors for the latex cast method (LCM) and the ellipse model method (EMM)

	Directional error <sup>a</sup>						Absolute error <sup>b</sup>					
	Femur 50%		Femur 80%		Tibia 50%		Femur 50%		Femur 80%		Tibia 50%	
	% error	SD <sup>c</sup>	% error	SD	% error	SD	% error	SD <sup>c</sup>	% error	SD	% error	SD
LCM												
TA	-2.0	2.9	-0.7	4.6	-0.1	3.9	3.0	2.2	3.6	2.7	3.2	2.4
MA	-9.8*	9.4	-8.6*	10.8	2.1	18.3	11.2	7.5	11.6	7.1	13.9	11.1
CA	0.5	3.8	4.3*	7.0	-0.4	7.2	3.3	2.3	6.8	4.2	5.4	4.7
I <sub>x</sub>	-3.6*	5.9	0.8	9.7	-1.1	7.2	5.9	4.1	7.5	5.7	6.1	4.5
I <sub>y</sub>	-3.3*	5.4	-0.7	9.6	0.1	8.9	5.3	4.2	7.7	5.9	7.1	5.5
I <sub>min</sub>	-4.2*	5.7	-1.8	9.7	-0.5	8.0	6.2	4.1	7.7	5.8	6.1	5.5
I <sub>max</sub>	-2.3*	5.6	3.5*	9.6	-1.3	7.6	5.2	3.8	7.8	6.0	6.5	4.8
J	-3.4*	5.5	0.1	9.3	-0.6	7.3	5.6	4.4	7.3	5.6	6.0	4.7
EMM												
TA	3.9*	5.7	-0.4*	6.9	4.9*	7.6	5.6	4.0	5.4	4.3	7.2	5.3
MA	-0.7*	9.4	-5.2*	11.7	-5.2*	10.0	6.9	6.3	9.8	8.2	8.9	6.8
CA	5.4*	6.7	2.6*	9.1	10.5*	11.8	6.8	5.2	7.5	5.7	12.0	10.3
I <sub>x</sub>	7.9*	13.1	0.5*	14.6	-4.0*	12.2	11.6	9.7	11.6	8.8	10.6	7.2
I <sub>y</sub>	4.8*	10.5	-8.6*	12.0	4.3*	17.5	9.4	6.6	9.4	8.2	14.4	10.7
J	6.3*	11.3	-4.5*	12.3	-0.9*	13.4	10.2	7.9	10.2	7.7	10.0	8.6

\*Paired *t*-tests between estimated and true properties; *p*-values were significant at  $\alpha = 0.05$ .

<sup>a</sup> directional % error = (estimated – true)/true·100.

<sup>b</sup> absolute % error = |(estimated – true)/true|·100.

<sup>c</sup> standard deviation of the mean % error.

Table 4

Multiple regression of true cross-sectional properties on properties estimated using the ellipse model method (EMM) and five independent variables

	CA			I <sub>x</sub>			I <sub>y</sub>			J		
	Slope <sup>a</sup>	SE <sup>b</sup>	p	Slope <sup>a</sup>	SE <sup>b</sup>	p	Slope <sup>a</sup>	SE <sup>b</sup>	p	Slope <sup>a</sup>	SE <sup>b</sup>	p
<i>Femur 50%</i>												
Sex <sup>c</sup>	-2.31	2.61	0.38	-4.32	5.12	0.40	-4.2	4.06	0.31	-11.75	8.07	0.15
Age	0.14	0.11	0.21	0.25	0.22	0.25	0.24	0.17	0.18	0.34	0.34	0.32
%CA <sup>d</sup>	0.25	0.19	0.20	0.70	0.38	0.07	0.29	0.30	0.34	0.86	0.60	0.16
I <sub>max</sub> /I <sub>min</sub>	2.18	5.28	0.68	1.29	10.37	0.90	4.54	8.22	0.58	14.80	16.36	0.37
θ	0.01	0.05	0.91	0.03	0.10	0.74	0.07	0.08	0.37	0.14	.16	.40
Femur Length	0.01	0.06	0.85	-0.03	0.11	0.77	0.01	0.09	0.94	-0.02	0.18	0.93
<i>Femur 80%</i>												
Sex <sup>c</sup>	-1.18	2.79	0.68	-8.43	5.26	0.87	-1.86	4.25	0.66	-1.45	4.35	0.74
Age	0.04	0.13	0.79	0.08	0.25	0.75	0.06	0.20	0.76	0.06	0.21	0.77
%CA <sup>d</sup>	-0.07	0.21	0.73	0.38	0.40	0.34	0.09	0.32	0.79	0.21	0.33	0.52
I <sub>max</sub> /I <sub>min</sub>	19.40	3.64	<b>0.000</b>	19.82	6.87	<b>0.006</b>	17.01	5.55	<b>0.004</b>	17.97	5.68	<b>0.003</b>
θ	0.07	0.13	0.59	0.09	0.25	0.73	-0.09	0.20	0.66	-0.05	0.21	0.83
Femur Length	-5.69	0.06	0.79	-4.49	0.12	0.71	-0.10	0.10	0.29	-0.08	0.10	0.46
<i>Tibia 50%</i>												
Sex <sup>c</sup>	-7.82	3.93	<b>0.053</b>	2.19	5.11	0.67	-15.74	6.00	<b>0.012</b>	-4.55	4.85	0.35
Age	0.05	0.16	0.76	0.22	0.21	0.29	0.33	0.24	0.18	0.25	0.20	0.21
%CA <sup>d</sup>	-0.50	0.19	<b>0.010</b>	-0.14	0.24	0.57	-0.80	0.28	<b>0.007</b>	-0.40	0.23	0.09
I <sub>max</sub> /I <sub>min</sub>	7.31	2.80	<b>0.012</b>	4.93	3.63	0.18	4.24	4.24	<b>0.32</b>	4.60	3.45	0.19
θ	-0.39	0.18	<b>0.042</b>	-0.10	2.40	0.69	-0.55	0.28	<b>0.055</b>	-0.36	0.23	0.12
Tibia Length	-0.11	0.07	0.15	-0.06	0.10	0.57	-0.19	0.11	0.10	-0.11	0.09	0.24

Boldface indicates *p*-value significant at  $\alpha = 0.05$ .

<sup>a</sup> Least squares slope.

<sup>b</sup> Standard error of the slope.

<sup>c</sup> Sex = males 1, females 0.

<sup>d</sup> %CA = (cortical area/total area)·100.

bones. The only section property with directional errors greater than 4% using this technique was MA, which is not surprising given that this property is the most dependent on the radiographic measurements and an assumed elliptical shape. From a mechanical perspective, MA is the least important section property, since it does not reflect rigidity or strength per se.

By contrast, although correlations are still strong and standard errors reasonable, the results from the EMM indicate that there is a bias in this method that results in overestimation of most cross-sectional properties. This suggests that results obtained using EMM and other methods (direct measurement, computed tomography, latex cast method) are often not equivalent and should not be combined unless a correction for the bias in EMM is performed. The correction formulae

generated herein appear to successfully adjust femoral midshaft section properties determined using the EMM, with resultant errors within the range of LCM errors, i.e.,  $\leq 4\%$ . However, attempts to correct the other two sections were less successful (except for CA), and so the above caution remains for these sections. The more mixed results for the femoral 80% and tibial 50% sections may be a consequence of the more marked effects of differences in section geometry— $I_{\max}/I_{\min}$ , theta, %CA—on EMM estimation error in these sections (Table 4). Therefore, our correction formulae will not be as effective in samples or individuals that differ from the Pecos Pueblo reference sample in these characteristics.

The only previous study to have tested the accuracy of the LCM is that of Stock (2002), in which a small sample ( $n = 7$ ) of canine tibiae were

Table 5

Multiple regression of true cross-sectional properties on properties estimated using the latex cast method (LCM) and five independent variables

	CA			$I_x$			$I_y$			J		
	Slope <sup>a</sup>	SE <sup>b</sup>	p	Slope <sup>a</sup>	SE <sup>b</sup>	p	Slope <sup>a</sup>	SE <sup>b</sup>	p	Slope <sup>a</sup>	SE <sup>b</sup>	p
<i>Femur 50%</i>												
Sex <sup>c</sup>	-0.86	1.46	0.56	-1.69	2.28	0.46	-1.11	2.09	0.60	-1.45	2.15	0.50
Age	-0.02	0.06	0.65	-0.17	0.10	0.09	-0.08	0.09	0.40	-0.13	0.09	0.17
%CA <sup>d</sup>	-0.01	0.11	0.97	-0.06	0.17	0.71	-0.08	0.16	0.63	-0.07	0.16	0.67
$I_{\max}/I_{\min}$	-0.82	2.96	0.78	-2.40	4.62	0.60	-2.34	4.24	0.58	-2.44	4.35	0.58
$\theta$	-0.01	0.03	0.98	-0.01	0.05	0.99	0.02	0.04	0.72	0.01	0.04	0.86
Femur Length	0.06	0.03	0.06	0.09	0.05	0.09	0.10	0.05	<b>0.042</b>	0.09	0.05	0.06
<i>Femur 80%</i>												
Sex <sup>c</sup>	-2.98	2.32	0.21	-0.06	3.56	0.99	-0.41	3.58	0.91	-0.17	3.46	9.6
Age	-0.11	0.11	0.34	-0.21	0.17	0.22	-0.20	0.17	0.24	-0.20	0.16	0.22
%CA <sup>d</sup>	-0.41	0.18	<b>0.026</b>	-0.19	0.27	0.49	-0.13	0.27	0.64	-0.16	0.26	0.56
$I_{\max}/I_{\min}$	8.01	3.03	<b>0.011</b>	9.12	4.65	0.06	8.06	4.67	0.09	8.54	4.52	0.07
$\theta$	0.42	0.11	<b>0.001</b>	0.44	0.17	<b>0.014</b>	0.43	0.17	<b>0.017</b>	0.42	0.17	<b>0.015</b>
Femur Length	-0.01	0.05	0.86	-0.02	0.08	0.80	0.01	0.08	0.90	-0.01	0.08	0.94
<i>Tibia 50%</i>												
Sex <sup>c</sup>	2.27	2.70	0.41	3.77	2.92	0.20	3.45	3.27	0.30	3.44	2.78	0.22
Age	-0.12	0.11	0.27	-0.07	0.12	0.56	-0.03	0.13	0.80	-0.06	0.11	0.58
%CA <sup>d</sup>	-0.39	0.13	<b>0.004</b>	-0.24	0.14	0.10	-0.54	0.15	<b>0.001</b>	-0.35	0.13	<b>0.010</b>
$I_{\max}/I_{\min}$	1.90	1.92	0.33	0.57	2.08	0.79	2.26	2.32	0.34	0.93	1.98	0.64
$\theta$	-0.06	0.13	0.62	-0.22	0.14	0.12	-0.40	0.15	<b>0.012</b>	-0.35	0.13	<b>0.011</b>
Tibia Length	0.12	0.05	<b>0.024</b>	0.11	0.06	0.06	0.10	0.06	0.13	0.10	0.05	0.07

Boldface indicates  $p$ -value significant at  $\alpha = 0.05$ .

<sup>a</sup> Least squares slope.

<sup>b</sup> Standard error of the slope.

<sup>c</sup> Sex = males 1, females 0

<sup>d</sup> %CA = (cortical area/total area)·100.

used to test the correspondence between estimated cross-sectional properties and those derived from directly sectioning the bones. Stock (2002) argued that the canine tibia is reasonably representative of a gracile human humerus in terms of bone size and shape. The absolute percent differences between the LCM and true cross-sectional properties in his study range from 1-6%, while those reported here have a slightly higher range, from 3-8% (except MA, 11-14%). The slightly worse results reported here are probably due to the less circular, more angular shape of the human long bones examined. Stock's canine tibiae had a mean  $I_{\max}/I_{\min}$  ratio of 1.12 (J. Stock, pers. comm.), compared to mean  $I_{\max}/I_{\min}$  ratios of 1.20-1.65 in our three sections. Nonetheless, our results, similar to those of Stock, generally support the originally hypothesized error

magnitude of approximately 5% for the LCM (Trinkaus and Ruff, 1989).

In contrast to the LCM, several studies have evaluated the accuracy of the EMM when applied to a variety of mammalian long bones and other skeletal elements. Biknevicius and Ruff (1992) tested the method's accuracy when applied to a sample of carnivore mandibular corpora and found that average directional and random errors ranged from 1-26% for areas and second moments of area. However, this may represent a "worst-case scenario" since mandibular cross sections are very strongly asymmetric and irregular (Biknevicius and Ruff, 1992). Runestad et al. (1993) found much less directional bias in a sample of relatively circular small mammalian femora and humeri measured near midshaft, although there was a

Table 6

Ordinary least-squares (OLS) prediction equations for estimating true cross-sectional properties from properties estimated using the ellipse model method (EMM)

Section	Equation <sup>a</sup>	CF <sup>b</sup>	Directional error <sup>c</sup>	
			Original Mean (range)	Corrected Mean (range)
Femur 50%	LN True TA = $0.862 \times$ LN Estimated TA + 0.805	1.001	7.0 (−0.7–13.8)	0.01 (−11.7–7.0)
	LN True CA = $0.823 \times$ LN Estimated CA + 0.979	1.002	13.3 (−0.6–27.4)	3.7 (−7.0–16.5)
	LN True I <sub>x</sub> = $0.862 \times$ LN Estimated I <sub>x</sub> + 1.268	1.006	18.1 (−0.5–34.9)	3.7 (−10.7–16.8)
	LN True I <sub>y</sub> = $0.875 \times$ LN Estimated I <sub>y</sub> + 1.150	1.004	13.2 (−12.7–30.9)	3.5 (−15.5–14.8)
	LN True J = $0.868 \times$ LN Estimated J + 1.304	1.005	15.9 (−5.4–32.9)	3.6 (−12.3–16.1)
Femur 80%	LN True TA = $0.943 \times$ LN Estimated TA + 0.361	1.002	3.6 (−0.2–14.4)	3.6 (−5.0–14.1)
	LN True CA = $0.846 \times$ LN Estimated CA + 0.867	1.004	10.5 (−3.1–18.1)	4.6 (−5.2–12.5)
	LN True I <sub>x</sub> = $0.910 \times$ LN Estimated I <sub>x</sub> + 0.879	1.010	−1.0 (−19.0–9.5)	−2.0 (−18.0–7.9)
	LN True I <sub>y</sub> = $0.962 \times$ LN Estimated I <sub>y</sub> + 0.468	1.009	8.1 (−7.6–20.9)	18.1 (2.5–31.0)
	LN True J = $0.942 \times$ LN Estimated J + 0.658	1.008	3.9 (−13.5–16.0)	8.0 (−8.2–19.7)
Tibia 50%	LN True TA = $0.840 \times$ LN Estimated TA + 0.909	1.002	15.2 (5.6–13.5)	4.7 (−3.4–13.2)
	LN True CA = $0.771 \times$ LN Estimated CA + 1.181	1.004	17.4 (6.3–30.4)	−0.7 (−10.0–8.7)
	LN True I <sub>x</sub> = $0.924 \times$ LN Estimated I <sub>x</sub> + 0.767	1.008	− <sup>d</sup>	− <sup>d</sup>
	LN True I <sub>y</sub> = $0.774 \times$ LN Estimated I <sub>y</sub> + 2.009	1.008	− <sup>d</sup>	− <sup>d</sup>
	LN True J = $0.866 \times$ LN Estimated J + 1.357	1.007	22.8 (2.1–36.8)	15.3 (−4.0–28.8)

<sup>a</sup> CA, cortical area in mm<sup>2</sup>; I<sub>x</sub> and I<sub>y</sub>, second moments of area in mm<sup>4</sup>; J, polar moment of area in mm<sup>4</sup>.

<sup>b</sup> Correction factor for detransformation bias, in which the detransformed units are multiplied by a “quasi-maximum likelihood estimator” (QMLE) (Smith, 1993; Ruff, 2003a).

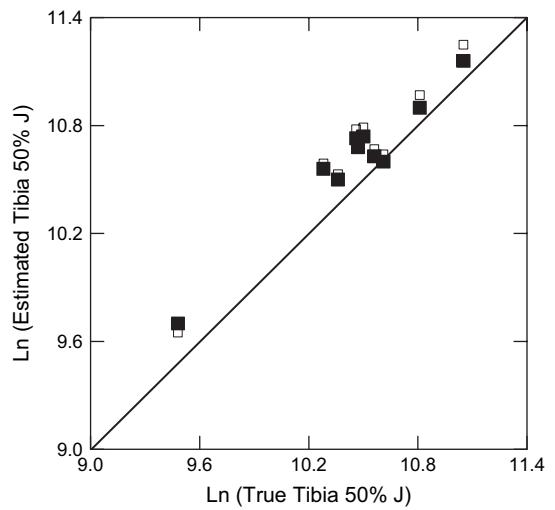
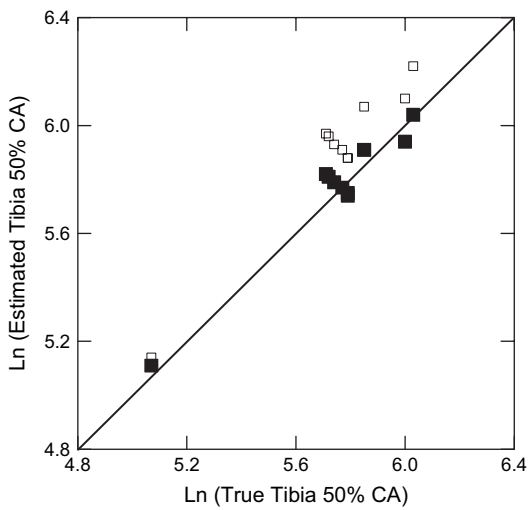
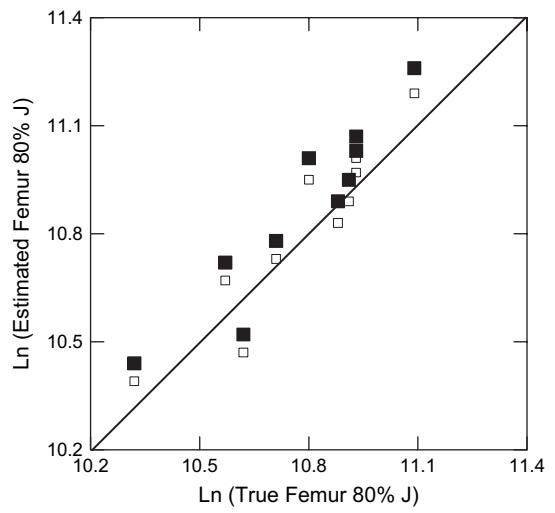
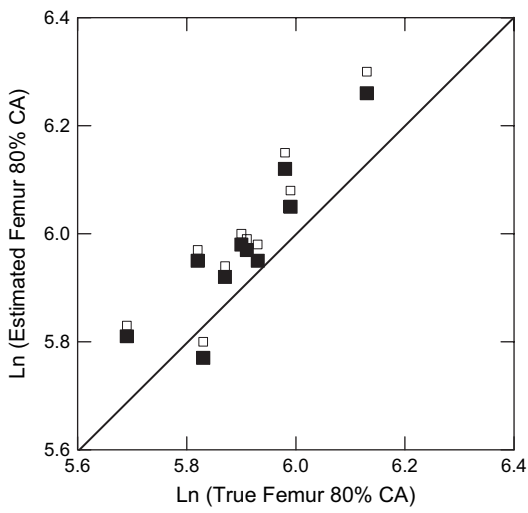
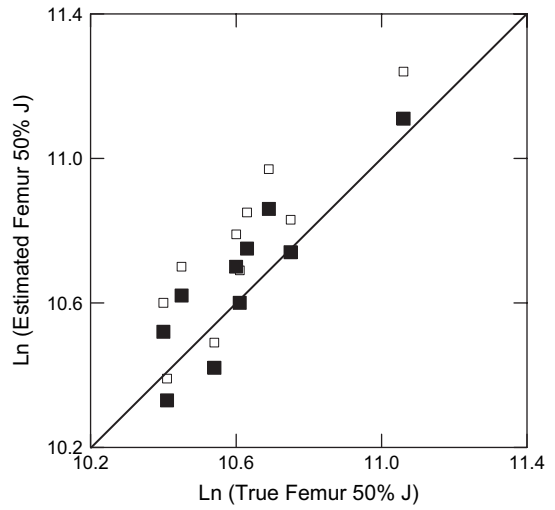
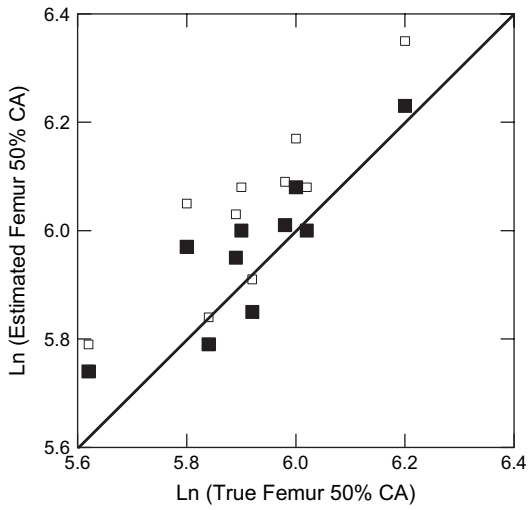
<sup>c</sup> Results from application of correction formulae to independent samples (see text).

<sup>d</sup> True I<sub>x</sub> and I<sub>y</sub> values not available for the original sample (Ruff and Hayes, 1988).

slight tendency to overestimate properties using the EMM. Fresia et al. (1990) found high correlations but a directional bias towards overestimation of properties using the EMM in human humeri measured in the mid-distal diaphysis. Additionally, there was little evidence for any size-related effect on errors. Overall then, these results are very similar to those found here for the human tibia and femur.

One possibility for improving the accuracy of EMM property estimates is to use the more complex eccentric ellipse model (EEM) (Milgrom et al., 1989; Ohman, 1993). However, the EEM has shown mixed levels of improvement over the EMM when applied to modern human long bones. For example, in a sample (n = 46) of human second metacarpals, Lazenby (1997) found only a very slight improvement in the EEM estimates of second moments of area compared to the EMM (I<sub>x</sub>: 4.6% vs. 5.7%; I<sub>y</sub>: 13.3% vs. 13.7% absolute errors). In a subsequent study using a much larger sample of metacarpals (n = 356) from the same

population, he found no difference between the EEM and EMM estimates of second moments of area (Lazenby, 1998). Similarly, Runestad et al. (1993) found no significant difference (as determined using regression statistics) between EEM and EMM property estimates. Ohman (1993) suggested that the EEM produced more accurate cross-sectional geometric property estimates in his sample of human and ape femora and humeri. However, his study did not include true cross-sectional properties with which to compare the EEM and EMM estimates. In order to evaluate the potential improvement of EEM relative to the EMM property estimates in the present sample, EEM properties for the same sections were computed using a Microsoft Excel macro written by the authors (available at: <http://www.hopkinsmedicine.org/FAE/CBR.htm>) and then compared to true values. On average, the percent estimation errors for the EMM and EEM were nearly equivalent. The mean directional and absolute EEM errors for second moments of area over all sections were



4.8% and 11.0%, respectively, which are actually slightly *greater* than the mean EMM errors of 4.3% and 10.7%, respectively. Stock (2002) observed similar error magnitudes for his eccentric ellipse models applied to canine tibiae, ranging from 6–14% for second moments of area. The only study to show a significant improvement in cross-sectional property estimates using the EEM vs. the EMM was a study of canine mandibular corpora (Biknevicius and Ruff, 1992), which are very strongly asymmetric. Therefore, there seems to be little empirical evidence that the EEM systematically improves cross-sectional property estimates in long bones. However, the EEM may be useful for strongly asymmetric sections, such as those obtained from mandibular corpora.

Lazenby (1998) carried out an error study in which he derived a series of regression equations for correcting the EMM estimates of section properties of the midshaft metacarpal in a skeletal sample of 19<sup>th</sup> century Eurocanadians. In a subsequent study that tested the utility of these proposed regression equations, Lazenby (2002) showed that the equations predicted good (unbiased) estimates of A-P and M-L second moments of area, which were not significantly different from the true parameters. However, his equations did not perform well when applied to estimates of CA and he did not provide equations for J. Furthermore, he apparently did not correct for radiographic image parallax before deriving his cross-sectional property estimates (Lazenby, 1998, 2002), which may result in an over-correction of EMM estimates if they are applied to values that have been parallax corrected. By contrast, the equations provided in Table 6 for the femoral midshaft sections significantly reduce the average directional errors in the test samples analyzed and improve the point estimates overall. There is no substantial difference in this section between the quality of improvement in the area and second moment of area estimates.

Overall, the multiple regression results suggest that more irregularly shaped sections with higher  $I_{\max}/I_{\min}$  ratios and less A-P or M-L oriented directions of greatest and least bending rigidity will have greater estimation error, particularly when using the EMM. These results are not surprising since they suggest that error will increase as true cross-sectional contours depart more from an assumed circle or regular ellipse oriented with its long and short axes in the A-P and M-L planes. Relatively thinner cortices also lead to more error, especially in the tibia. Thin cortices probably exacerbate error in non-circular sections because they tend to produce medullary contours that more closely parallel the (non-circular) subperiosteal contour. It is not possible to include these additional factors in EMM correction formulae, since they require knowledge of true section properties that would not be available. However, as noted above, our results do argue for caution in comparing results across samples that vary significantly in these characteristics, especially in the less circular proximal femur and midshaft tibia.

## Conclusions

In the human femur and tibia, cross-sectional properties derived using both the ellipse model and latex cast methods are highly correlated with true properties, with random (absolute) estimation errors averaging 3–8% for the LCM and only slightly higher, 5–14%, for the EMM. However, the EMM shows a systematic bias towards over-estimation of section properties, while directional bias is generally small for the LCM (except for MA in some sections). Thus, the LCM may be used with confidence to estimate section properties, while properties derived using the EMM should not be compared with those derived using more exact methods. However, femoral midshaft properties estimated using the EMM can be corrected using the formulae provided herein,

---

Figure 3. Scatter plots of the pooled Georgia coast Amerindian (i.e., femur 50%, 80%) and Euroamerican (i.e., tibia 50%) skeletal test samples showing cross-sectional property estimates before (empty squares) and after (solid squares) adjustment using the prediction equations in Table 6. All data transformed to natural logarithms. The solid line demonstrates equivalence between the estimated and true properties.

after which they may be included in such comparisons. In general, estimation errors can be expected to increase as sections become less circular and more obliquely oriented, and, at least for the tibial midshaft, develop thinner cortices. These errors are more pronounced in the EMM than in the LCM.

### Acknowledgements

This study was supported by the Johns Hopkins University School of Medicine. We thank Dr. J. Stock for kindly lending us his canine tibiae data, Dr. J. Ohman for a copy of his program GEO-XRAY and discussions regarding its implementation, and three anonymous reviewers whose comments improved the quality of the manuscript.

### References

- Altman, D.G., Bland, M.J., 1983. Measurement in medicine: the analysis of method comparison studies. *Statistician* 32, 307–317.
- Biknevicius, A.R., Ruff, C.B., 1992. Use of biplanar radiographs for estimating cross-sectional geometric properties of mandibles. *Anat. Rec.* 232, 157–163.
- Bland, M.J., Altman, D.G., 1986. Statistical methods for assessing agreement between two methods of clinical measurement. *Lancet* 1, 307–310.
- Churchill, S.E., 1994. Human upper body evolution in the Eurasian later Pleistocene. Ph.D. Dissertation, University of New Mexico.
- Churchill, S.E., Smith, F.H., 2000. A modern human humerus from the early Aurignacian of Vogelherdhohle (Stetten, Germany). *Am. J. Phys. Anthropol.* 112, 251–273.
- Counour, J.R., Glander, K., Vincent, F., 2000. Postcranial adaptations for leaping in primates. *J. Zool., Lond.* 251, 79–103.
- Fresia, A., Ruff, C.B., Larsen, C.S., 1990. Temporal decline in bilateral asymmetry of the upper limb on the Georgia coast. *Anthrop. Papers Am. Mus. Nat. Hist.* 68, 121–132.
- Holt, B.M., 2003. Mobility in Upper Paleolithic and Mesolithic Europe: evidence from the lower limb. *Am. J. Phys. Anthropol.* 122, 200–215.
- Hooton, E.A., 1930. The Indians of Pecos Pueblo: a study of their skeletal remains. *Papers of the Phillips Academy Southwestern Expedition*, vol. 4. Yale University Press, New Haven.
- Kidder, A.V., 1958. Pecos, New Mexico: Archaeological Notes. Phillips Academy, Andover, MA.
- Lazenby, R.A., 1997. Bias and agreement for radiogrammetric estimates of cortical bone geometry. *Invest. Radiol.* 32, 12–18.
- Lazenby, R.A., 1998. Second metacarpal geometry: rehabilitating a circular argument. *Am. J. Hum. Biol.* 10, 747–756.
- Lazenby, R.A., 2002. Prediction of cross-sectional geometry from metacarpal radiogrammetry: a validation study. *Am. J. Hum. Biol.* 14, 74–80.
- Milgrom, C., Giladi, M., Simkin, A., Rand, N., Kedem, R., Kashtan, H., Stien, M., Gomori, M., 1989. The area moment of inertia of the tibia: a risk for stress fractures. *J. Biomech.* 22, 1243–1248.
- Nagurka, M.L., Hayes, W.C., 1980. An interactive graphics package for calculating cross-sectional properties of complex shapes. *J. Biomech.* 13, 59–64.
- Ohman, J.C., 1993. Computer software for estimating cross-sectional geometric properties of long bones with concentric and eccentric elliptical models. *J. Hum. Evol.* 25, 217–227.
- Ruff, C.B., 1981. A reassessment of the demographic estimates for Pecos Pueblo. *Am. J. Phys. Anthropol.* 65, 347–358.
- Ruff, C.B., 1989. New approaches to structural evolution of limb bones in primates. *Folia Primatol.* 53, 142–159.
- Ruff, C.B., 1995. Biomechanics of the hip and birth in early *Homo*. *Am. J. Phys. Anthropol.* 98, 527–574.
- Ruff, C.B., 1999. Skeletal structure and behavioral patterns of prehistoric Great Basin populations. In: Hemphill, B.E., Larsen, C.S. (Eds.), *Understanding Prehistoric Lifeways in the Great Basin Wetlands: Bioarchaeological Reconstruction and Interpretation*. University of Utah Press, Salt Lake City, pp. 290–320.
- Ruff, C.B., 2000. Body size, body shape, and bone strength in modern humans. *J. Hum. Evol.* 38, 269–290.
- Ruff, C.B., 2003a. Long bone articular and diaphyseal structure in Old World monkeys and apes, II: body mass estimation. *Am. J. Phys. Anthropol.* 120, 16–37.
- Ruff, C.B., 2003b. Growth in bone strength, body size, and muscle size in a juvenile longitudinal sample. *Bone* 33, 317–329.
- Ruff, C.B., 2003c. Ontogenetic adaptation to bipedalism: age changes in femoral to humeral length and strength proportions in humans, with a comparison to baboons. *J. Hum. Evol.* 45, 317–349.
- Ruff, C.B., Hayes, W.C., 1983a. Cross-sectional geometry of Pecos Pueblo femora and tibiae—a biomechanical investigation: I. Method and general patterns of variation. *Am. J. Phys. Anthropol.* 60, 359–381.
- Ruff, C.B., Hayes, W.C., 1983b. Cross-sectional geometry of Pecos Pueblo femora and tibiae—a biomechanical investigation: II. Sex, age, and side differences. *Am. J. Phys. Anthropol.* 60, 383–400.
- Ruff, C.B., Hayes, W.C., 1988. Sex differences in age-related remodeling of the femur and tibia. *J. Orthop. Res.* 6, 886–896.
- Ruff, C.B., Larsen, C.S., Hayes, W.C., 1984. Structural changes in the femur with the transition to agriculture on the Georgia coast. *Am. J. Phys. Anthropol.* 64, 125–136.

- Ruff, C.B., Trinkaus, E., Walker, A., Larsen, C.S., 1993. Postcranial robusticity in *Homo*, I: temporal trends and mechanical interpretation. *Am. J. Phys. Anthropol.* 91, 21–53.
- Ruff, C.B., Walker, A., Trinkaus, E., 1994. Postcranial robusticity in *Homo*, III: ontogeny. *Am. J. Phys. Anthropol.* 93, 35–54.
- Runestad, J.A., 1997. Postcranial adaptations for climbing in Loridae (Primates). *J. Zool., Lond.* 242, 261–290.
- Runestad, J.A., Ruff, C.B., Nieh, J.C., Thorington, R.W., Teaford, M.F., 1993. Radiographic estimation of long bone cross-sectional geometric properties. *Am. J. Phys. Anthropol.* 90, 207–213.
- Sakaue, K., 1998. Bilateral asymmetry of the humerus in Jomon people and modern Japanese. *Anthropol. Sci.* 105, 231–246.
- Smith, R.J., 1993. Logarithmic transformation bias in allometry. *Am. J. Phys. Anthropol.* 90, 215–228.
- Smith, R.J., 1994. Regression models for prediction equations. *J. Hum. Evol.* 26, 239–244.
- Stock, J.T., 2002. A test of methods of radiographically deriving long bone cross-sectional geometric properties compared to direct sectioning of the diaphysis. *Int. J. Osteoarchaeol.* 12, 335–342.
- Stock, J., Pfeiffer, S., 2001. Linking structural variability in long bone diaphyses to habitual behaviors: foragers from the southern African Later Stone Age and the Andaman Islands. *Am. J. Phys. Anthropol.* 115, 337–348.
- Sumner, D.R., Mockbee, B., Morse, K., 1985. Computed tomography and automated image analysis of prehistoric femora. *Am. J. Phys. Anthropol.* 68, 225–232.
- Trinkaus, E., 1997. Appendicular robusticity and the paleobiology of modern human emergence. *Proc. Natl. Acad. Sci.* 94, 13367–13373.
- Trinkaus, E., Ruff, C.B., 1989. Diaphyseal cross-sectional morphology and biomechanics of the Fond-de-Forêt 1 femur and the Spy 2 femur and tibia. *Bull. Soc. Roy. Bel. Anthropol. Préhist.* 100, 33–42.
- Trinkaus, E., Ruff, C.B., 1999a. Diaphyseal cross-sectional geometry of Near Eastern Middle Palaeolithic humans: the femur. *J. Archaeol. Sci.* 26, 409–424.
- Trinkaus, E., Ruff, C.B., 1999b. Diaphyseal cross-sectional geometry of Near Eastern Middle Palaeolithic humans: the tibia. *J. Archaeol. Sci.* 26, 1289–1300.
- Trinkaus, E., Churchill, S.E., Ruff, C.B., 1994. Postcranial robusticity in *Homo*, II: humeral bilateral asymmetry and bone plasticity. *Am. J. Phys. Anthropol.* 93, 1–34.
- Trinkaus, E., Ruff, C.B., Churchill, S.E., 1998a. Upper limb versus lower limb loading patterns among Near Eastern Middle Paleolithic hominids. In: Akazawa, T., Aoki, K., Bar-Yosef, O. (Eds.), *Neandertals and Modern Humans in West Asia*. Plenum Press, New York, pp. 391–404.
- Trinkaus, E., Ruff, C.B., Churchill, S.E., Vandermeersch, B., 1998b. Locomotion and body proportions of the Saint-Césaire 1 Châtelperronian Neandertal. *Proc. Natl. Acad. Sci.* 95, 5836–5840.
- Trinkaus, E., Stringer, C.B., Ruff, C.B., Hennessy, R.J., Roberts, M.B., Parfitt, S.A., 1999. Diaphyseal cross-sectional geometry of the Boxgrove 1 middle Pleistocene human tibia. *J. Hum. Evol.* 37, 1–25.
- Wainwright, S.A., Biggs, W.D., Currey, J.D., Gosline, J.M., 1976. *Mechanical Design in Organisms*. Halsted Press, New York.
- Zabecki, M., O'Neill, M.C., Ruff, C.B., 2004. Relative bone strength in the upper and lower limbs of a Predynastic Egyptian population. *Am. J. Phys. Anthropol.* 38 (Suppl.), 214–215.